Optimal Control Joint Design of Large-Tip-Angle RF Pulses and Gradient Waveforms for Parallel Transmission

Weiran Deng[1], Benedikt Poser[1], and V Andrew Stenger[1]
[1]*Department of Medicine, University of Hawaii JABSOM, Honolulu, HI, United States*

Abstract: Conventional parallel transmission RF pulse design [1] uses predetermined k-space trajectories and computes the RF pulse by solving an ill-posed problem. The joint design method simultaneously computes the RF pulse and optimizes for a better k-space trajectory from the predetermined one [2,3]. However, the linear joint design approach is based on the Small Tip Approximation (STA) [4] and is not accurate for large tip angle RF pulses. We present a nonlinear joint design method using optimal control theory for large tip angle parallel transmission RF pulse design. Bloch equation simulations are performed for accuracy comparisons.

Theory: Optimal control theory [5,6] uses the RF pulse $\boldsymbol{b_1}(t) = b_x(t) + ib_y(t)$ and gradient $\boldsymbol{g}(t) = [g_x(t)\ g_y(t)\ g_z(t)]^T$ as control variables to steer the magnetization from the initial state to a desired magnetization pattern by minimizing a performance index $\boldsymbol{J}$:

$$J(b_1,\boldsymbol{g}) = \left\|\boldsymbol{M}(T) - \boldsymbol{D}\right\|^2 + \int_0^T H\{b_1,\boldsymbol{g},t\}\,dt.$$

$\boldsymbol{M}(T)$ is the final magnetization, $\boldsymbol{D}$ is the desired magnetization, and H the Hamiltonian $H = L + \boldsymbol{\lambda}^T\boldsymbol{f} + \boldsymbol{\mu}^T\boldsymbol{h}$ where $\boldsymbol{\lambda}$ and $\boldsymbol{\mu}$ are Lagrange multipliers for constraints. H includes a soft constraint L on the total RF power, a hard constraint $\boldsymbol{h}$ on the gradient amplitude, and a hard constraint $\boldsymbol{f}$ defined by the non-linear Bloch equation. $\boldsymbol{f}$ is only effective when the maximum gradient amplitude is reached.

Methods: A four-spoke "fast-k_z" 3D trajectory 2x under-sampled for eight parallel transmitters was used for demonstration (gradient amplitude=40mT/m, peak slew rate=125mT/m/s, 8.38ms pulse length). The desired excitation pattern was an 11×11cm square with a 90° tip angle at the center of a 22×22cm field of view. The initial pulse was estimated by the STA and used in the forward Bloch simulation to find $\boldsymbol{M}(t)$. The Lagrange multiplier was integrated from $\boldsymbol{\lambda}(T)=\boldsymbol{D}$ backward to find $\boldsymbol{\lambda}(T)$. $\boldsymbol{M}(t)$ and the $\boldsymbol{\lambda}(t)$ were then used to update the RF and the gradient waveform using a steepest descent algorithm. The gradient waveform was checked each iteration to enforce the peak slew rate. The iteration stopped when the improvement of excitation accuracy was less than 1E-3. Fig. 1a shows simulated eight-channel B_1^+ profile and 1b shows the RF magnitude and phase of the first channel. Fig. 2a shows the predetermined k-space trajectory and 2b shows the jointly optimized trajectory.

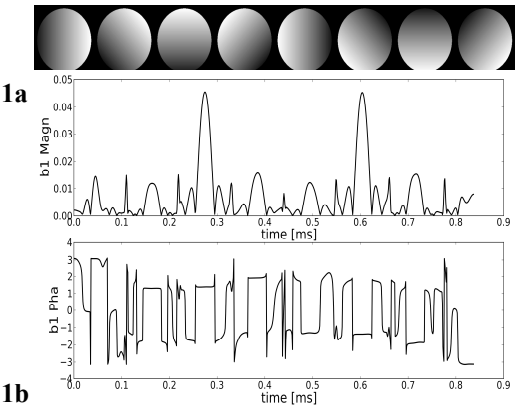

1a 1b

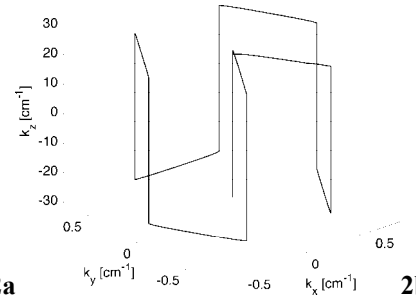

2a

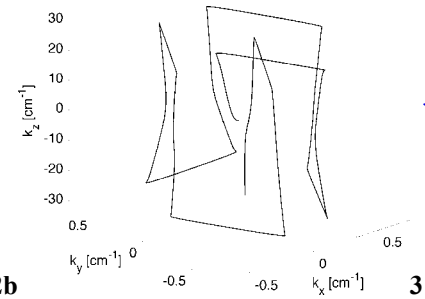

2b

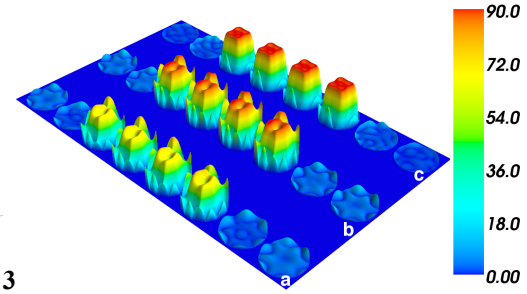

3

Results: The joint optimal control design was compared to the STA and an optimal control design for the RF pulse alone. The computing time of the joint optimization was 220 seconds. The pulses were simulated for eight slices with a 256×256 resolution. The 3D excitation profiles are shown in Fig. 3 for all eight slices. Fig. 3a shows the STA profile, 3b the profile from the RF optimal control design, and 3c from the joint optimal control design. Comparing the excitation error defined as the sum of the difference between the actual excitation and the desired excitation, the joint optimal control design showed 28% improvement over the conventional optimal control design, and 33% improvement over the STA design.

Conclusion: Joint optimization of the RF pulse and the gradient waveform using optimal control theory was shown to effectively improve excitation accuracy at a penalty of longer computing time. This design strategy can be extended to the design of other pulses such as 2D spiral and spatial-spectral pulses.

References: [1] Grissom et al, Magn Reson Med 2006;56:620-62. [2] Yip et al, Magn Reson Med 2007;58:598-604. [3] Ma et al, Magn Reson Med 2011;64:973-985. [4] Pauly et al, J Magn Reson 1989;81:43-56. [5] Connolly et al, IEEE Trans Med Imaging 1986;5(2):106-115. [6] Xu et al, Magn Reson Med 2008;59:547-560.

Acknowledgments: Work supported by the NIH (R01DA019912, R01EB011517, K02DA020569). Core resources supported by the NCRR (G12-RR003061, P20-RR011091), NINDS (U54-NS56883), and the ONDCP.